Zinc accelerates respiratory burst termination in human PMN

Annika Droste [a,d,1], Gustavo Chaves [a,1], Stefan Stein [b], Annette Trzmiel [b], Matthias Schweizer [c], Hubert Karl [f], Boris Musset [a,e,*]

[a] *Center of Physiology, Pathophysiology and Biophysics, Paracelsus Medical University, Nuremberg, Germany*
[b] *Flow Cytometry Unit, Institute for Tumor Biology and Experimental Therapy, Georg-Speyer-Haus, Frankfurt, Germany*
[c] *Federal Institute for Vaccines and Biomedicines, Paul-Ehrlich-Institut, Langen, Germany*
[d] *Department of Gynecology and Obstetrics, Johannes Gutenberg University, Mainz, Germany*
[e] *Center of Physiology, Pathophysiology and Biophysics, Paracelsus Medical University, Salzburg, Austria*
[f] *Department efi, Technische Hochschule Nürnberg Georg Simon Ohm, Nuremberg, Germany*

ABSTRACT

The respiratory burst of phagocytes is essential for human survival. Innate immune defence against pathogens relies strongly on reactive oxygen species (ROS) production by the NADPH oxidase (NOX2). ROS kill pathogens while the translocation of electrons across the plasma membrane via NOX2 depolarizes the cell. Simultaneously, protons are released into the cytosol. Here, we compare freshly isolated human polymorphonuclear leukocytes (PMN) to the granulocytes-like cell line PLB 985. We are recording ROS production while inhibiting the charge compensating and pH regulating voltage-gated proton channel (H_V1). The data suggests that human PMN and the PLB 985 generate ROS via a general mechanism, consistent of NOX2 and H_V1. Additionally, we advanced a mathematical model based on the biophysical properties of NOX2 and H_V1. Our results strongly suggest the essential interconnection of H_V1 and NOX2 during the respiratory burst of phagocytes. Zinc chelation during the time course of the experiments postulates that zinc leads to an irreversible termination of the respiratory burst over time. Flow cytometry shows cell death triggered by high zinc concentrations and PMA. Our data might help to elucidate the complex interaction of proteins during the respiratory burst and contribute to decipher its termination.

1. Introduction

The innate immune system is the first line of defence against pathogens in the human body. Phagocytes are the cells that represent the evolutionary oldest part of the whole immune system [1,2]. Even in humans with their active adaptive immune system the innate immune system is highly effective. One major part of the dynamic immune defence of phagocytes is the generation of reactive oxygen species (ROS) [3]. An enzyme complex called NADPH oxidase is translocating electrons across the phagosomal membrane into the phagosome [4]. There, molecular oxygen is reduced to superoxide (O_2^-). Superoxide reacts with protons to produce hydrogen peroxide (H_2O_2) which may then be converted to hypochlorous acid by myeloperoxidase and free chloride [5–7]. The hypochlorous acid is a bactericide substance that kills most of the pathogens invading the human body. However, the selective translocation of charge particles across a double lipid layer generates a

current and an electrical potential across the membrane [8]. If the charge is compensated by a counter charge, this then balances the net charge movement across the membrane and the electrical potential across the membrane equilibrates. In human phagocytes the voltage-gated proton channel (hH_V1) is the main charge compensator. The voltage-gated proton channel (H_V1) selectively conducts protons [9] through the membrane, driven by the electrochemical gradient. H_V1 is opened by depolarization of the membrane and acidification of the cytosol [10]. It is strongly expressed in phagocytes in intracellular membranes and the plasma membrane [11–17]. The NADPH oxidase (NOX2) produces free protons in the cytosol by oxidizing NADPH. The protons swiftly bind to water and hydronium ions accumulate in the cytosol lowering the intracellular pH (pH$_i$). Both low pH$_i$ and strong depolarization are inhibiting the NOX2 isoforms [18–21]. Therefore, H_V1 is the optimal partner to compensate for the chemical and electrical products originating from NOX2 [22]. The inhibition of ROS production

by phagocytes is highly reproducible via zinc ions [16,19,23]. Zn^{2+} is a very potent inhibitor of H_V1 function [24]. Zinc binds to the external part of the proton channel protein and prevents the channel from gating into an open configuration [25–28]. At an external pH = 7.0 zinc inhibits H_V1 at concentrations around 1 μM [29]. Interestingly, in patch-clamp experiments, where membrane potential is controlled by the patch-clamp amplifier, zinc concentrations up to 3 mM do not inhibit NOX2 function noticeably [19,30]. Accordingly, ROS production in phagocytes is inhibited by zinc not directly by affecting NOX2 but indirectly via strong depolarization. The effector is H_V1.

In the human body, zinc concentrations up to 1.6 mmol/l are found in seminal fluid [31], contributing to the low activity of immune cells in the testis. Zinc is concentrated in the insulin vesicles of the β-cells, composing hexamers of insulin. Surprisingly, H_V1 contributes to insulin release from β-cells, and if it is missing, is suspected to lead to glucose intolerance [32]. In tissues of the eye extraordinary high amounts of zinc per gram tissue have been measured [33,34]. Testis and the eye are known to be immune privileged, having reduced immune cell activity and quantity. Zinc reduces the activity of immune cells [19,23,35–40]. Thus, zinc appears to be a natural regulator of the immune response [41] which is often linked to H_V1 function. A designed peptide inhibitor, targeting the zinc binding sites of H_V1, was able to potently reduce ROS production in human white blood cells [42]. The peptide inhibitor underscores the function of H_V1 as well as zinc during the respiratory burst.

It has been discussed in detail which factors prolong or terminate the respiratory burst in phagocytes [43]. Especially, four factors have been suspected to be responsible for the termination of the respiratory burst: H_2O_2 has been suggested, actin has been suggested being essential for cytoskeletal motion [44], the regulatory GTPase Rac is involved in termination of the respiratory burst [45,46], and the phosphorylation status [47]. These appear to be the main four players. However, many mechanisms are still under discussion, two of them might be proposed by zinc inhibition experiments: cytosolic pH and membrane potential. While the pH would affect the entire cell, the effect of strong depolarization will be located at the membrane. Interestingly, it is unknown how chelating the zinc from H_V1 during the respiratory burst affects ROS production. Teleologically, is the effect of zinc inhibition reversible or permanent?

Here, we have measured ROS production of freshly isolated human polymorphonuclear leucocytes (PMN) and from four human cell lines (SBW [NOX2 knock-out, BFP labelled], SgpsIBW [reintroduced NOX2 gene, BFP labelled], PLB985 [wildtype control], X-CGD [NOX2 knock-out]). We were able to prove that inhibition of H_V1 by zinc had qualitatively the same effect in native cells as in the cell lines. ROS production in leucocytes is mainly due to NOX2. The NOX2 knock out cell line X-CGD had a miniscule production of ROS. Zinc inhibition was removed by adding pH buffered EGTA solution. Zinc chelating experiments showed that phagocytes ROS production recovered. However, the longer the zinc inhibition lasted the lesser was the recovery of ROS production. The mathematical model from Murphy and DeCoursey 2006 [8] was refined by adding a Posicast function. The model plus Posicast reproduces the experimental data of H_2O_2 release well. We propose that inhibition of H_V1 by zinc results in respiratory burst termination. Cell membrane integrity measurements via flow cytometry showed enhanced cell death due to the phorbol ester (PMA) and high zinc concentrations.

2. Material and methods

2.1. PMN isolation

Venous blood was drawn from healthy adult volunteers under the informed consent according to procedures approved by the Institutional Review Board at the Paracelsus Medical University, Nuremberg, Germany. Blood was diluted with PBS and PMN were purified following the publication of Boyum, 1968 [48]. PMN were directly counted and suspended in Ringer (in mmol/l: 160 NaCl, 4.5 KCl, 2 CaCl$_2$, 1 MgCl$_2$, 5

HEPES, pH 7.4//Osmolarity 300 mOsmol/l).

Solutions were modified to be phosphate free. Phosphate binds Zn^{2+} with high affinity, $Zn_3(PO_4)_2$ which is almost insoluble [49]. Thereby, we omitted PO_4^{3-} as it could potentially affect our zinc inhibition assays.

2.2. PLB985 culture and differentiation

Cells were kept in a standard incubator at 37 °C and 5% CO$_2$ in regular RPMI 1640 GlutaMAX 10% FBS. Splitting was performed when cell density reached 3.5×10^5 cells/ml every 2–3 days. It appeared that self-induced differentiation of the cells started at cell density of 10^6 cells/ml. All cell lines were treated identically. Differentiation was performed utilizing DMSO 1.25% (v/v) and reduced FBS content to 2.5%. After six days, cells were resuspended in Ringer in the desired concentration and prepared for H_2O_2 measurement. The following cell lines were tested: PLB 985 [50], X-CGD = knock-out of NOX2 in PLB985 [51], SBW = X-CGD cell line expressing BFP (blue fluorescent protein), SgpsIBW = X-CGD cell line co-expressing BFP and NOX2 [52].

2.3. Amplex Red assay quantification of H_2O_2 production

H_2O_2 release was measured using Amplex ultra red (Invitrogen® A36006) which is catalysed by horseradish peroxidase (HRP) to the fluorescent and stable resorufin. The catalysed reaction between Amplex Red molecule and H_2O_2 has a stoichiometry of 1:1, one mol H_2O_2 produces one mol Resorufin. Therefore, quantification of H_2O_2 production is possible. Measurements were done in a volume of 100 μl, with typically 2.5×10^4 cells/well. However, data normalized to one cell is displayed to increase comparability between experiments. Absolute concentrations of H_2O_2 were taken in each experiment from a freshly made calibration curve. Zn^{2+} in the concentrations experimentally applied did not affect the calibration curve. Measurements were done at 37 °C after brief shaking for 1 min. A dose response curve of phorbol 12-myristate 13-acetate (PMA) concentration compared to ROS production was generated. Highest production of ROS was achieved at a concentration of 120 nM PMA in the well. PMA was dissolved in 1:1 DMSO and Ethanol volume. Each recording was done in doublets to reduce possible sources of errors. The number of experiments (n) refers to independent individual experiments and does not refer to assay repeats with the same cells.

2.4. Quantification of cell death by flow cytometry

Plasma membrane integrity as marker for cell death was assessed by the DNA-binding dye propidium iodide (PI). After incubation of the cells with 40 ng PI (Thermo Fisher Scientific 00-6990) for 5 min, incorporation was measured using a FACSCanto II (BD Heidelberg, Germany). Measurements were done in triplicates and analyzed for PI positive cells within the BFP expressing population using FACSDiVa 6.1.3 and FlowJo 10.7.

2.5. Matlab mathematical model

We transformed the model of Murphy and DeCoursey [8] into Matlab R2018b 64 bit and its toolbox Simulink 9.2. We were able to reproduce the data presented in the publication. To convert electron current to H_2O_2 release, we integrated the electron current and plotted the data into a H_2O_2 time plot. Data was multiplied by 0.5 based on the redox reaction of two electrons forming one H_2O_2.

In the Murphy and DeCoursey model the electron current (Ie) is running into a constant value (10 pA). This would result into the integral:

$$\lim_{t \to \infty} \int_{\tau=0}^{\tau=t} I_e(\tau)\,\mathrm{d}\tau = \infty \qquad (1)$$

Introduction of a factor reducing *Ie* can be expressed as a so called Posicast function, which contents a Laplace transfer function

$$G_P(s) = 1 - e^{-sTt} \qquad (2)$$

where.

    $s \varepsilon \mathbb{C}$ = the Laplace variable with the unit 1/sec
    Tt = dead time in seconds

Over time the electron current *Ie* runs into a constant but finite value Ie_{konst}. The output of the Posicast transfer function can be expressed as:

$$\lim_{t\to\infty} Ie, out(t) = \lim_{s\to 0} s * Ie, out(s) = \lim_{S\to 0} s * \left(1 - e^{-sTt}\right)(1/s)\, Ie_{konst} = 0 \qquad (3)$$

Or as:

$$\int_0^t Ie, out\,(\tau)d\tau = \int_0^{Tt} Ie, out(t)dt \leq M \ < \infty... \Big/\!\!\Big/\!\!\Big/\!\!\Big/ \text{ applies for } t \geq Tt \qquad (4)$$

The data was later scaled to the experimental data by filter function:

$$G_F(s) = K_p \frac{sT + 1}{s\tau + 1} \qquad (5)$$
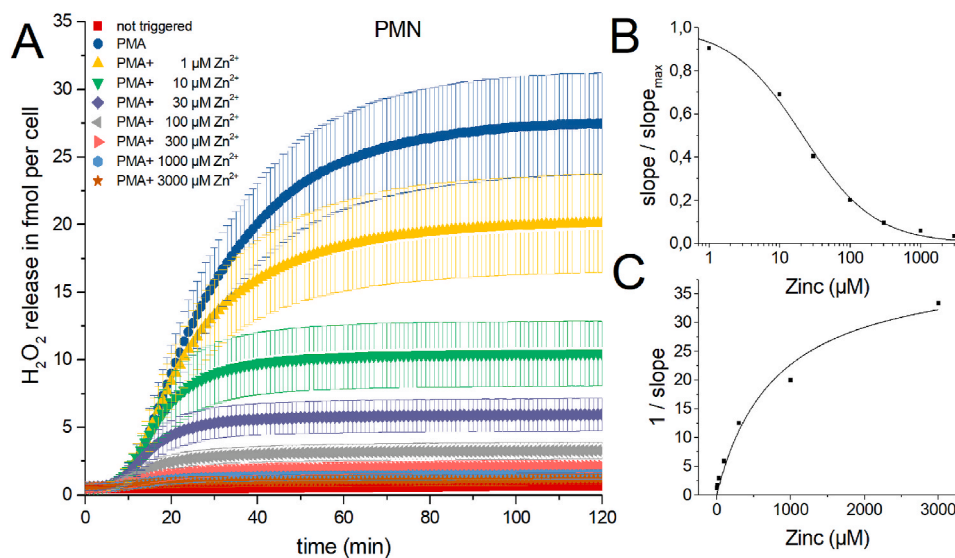
    Kp = proportional coefficient
    T = time constant in seconds
    τ = time constant in seconds

3. Results

3.1. PMN data

In freshly isolated human PMN, respiratory burst was initiated by 120 nM of the phorbol ester PMA [53]. After a brief initial delay (2–4 min) human PMN start producing H_2O_2 at an increasing rate (Fig. 1). Concentrations of zinc from 1 μM to 3 mM were added to the cells before mixing and PMA activation. During the course of the experiment, substantial inhibition of the ROS production by zinc was visible. Over the whole 120 min two phases of production emerge. There is an initial phase after the delay showing strong production. In most traces shown in Fig. 1, after 20 min the first phase transitioned into a second phase where the slope of the production is shallow or absent. Inhibition by zinc is instantly visible at t = 90 min as a clear reduction of overall released

H_2O_2. Initial production is best seen as the steepness of the slope of cumulative hydrogen peroxide production, or as the maximum of the first derivative of the cumulative H_2O_2 release. The slope of production (production rate) is decreasing with increasing zinc concentrations (Fig. 1B). An inhibition of 50% of the H_2O_2 release (fmol • min^{-1} • $cell^{-1}$) resulted in an IC_{50} of 21 μM Zn^{2+}. Overall, zinc inhibits potently the release of H_2O_2 by PMN. The Dixon plot of Fig. 1C shows an almost linear reduction of H_2O_2 release up to 100 μM of Zn^{2+}, suggesting an apparent αK_i of 28 μM. However, αK_i is exclusively deductible from the data, if the inhibition researched is a noncompetitive inhibition and substrate levels are saturating. Zinc binds to H_V1 not to NOX2 which literally represents noncompetitive inhibition, where the NOX2 would represent the enzymatic active site and H_V1 would be a binding position distant to the active site, albeit affecting the active site. Virtually, the substrate for H_2O_2 is NADPH which we are certain is at saturating levels during the respiratory burst in the PMN.

3.2. Data PLB985

There are cell lines that represent human PMN and are generally used in respiratory burst research if freshly isolated human PMN are not available or intended to be used. PLB985 cells are similar to the HL-60 cell line derived from a patient with acute myeloid leukemia [50]. We compared the respiratory burst of PLB985 cells with the human PMN by repeating zinc inhibition experiments. Firstly, we focused on the functional comparability of PMN to PLB985. The results would then indicate whether the dualism of NADPH oxidase and the voltage-gated proton channel is a general principle of ROS release during the oxidative burst. To produce quantifiable amounts of H_2O_2, PLB985 cells had to be differentiated over 5–7 days. Fig. 2 shows the sum of 5 recordings of differentiated PLB985 cells.

Qualitatively zinc has the same effect on PLB985 respiratory burst as in freshly isolated human PMN. The IC50 = 33 μM Zn^{2+} and apparent KM = 751 μM Zn^{2+}, which is reasonably close to PMN. However, there are some fine differences. The delay before visible onset of H_2O_2 release is prolonged compared to PMN. We reasoned that the differentiation process does not fully differentiate all PLB985 cells into granulocytes. Preliminary states of differentiation and undifferentiated cells are most likely still part of the population of the recorded cells [54]. As a population effect we would see this variability in differentiation as a delay in the onset of production. One more difference is that PMN were isolated from erythrocytes by osmotic shock, which was not applied to PLB cells. The standard error of the H_2O_2 release is much more pronounced in

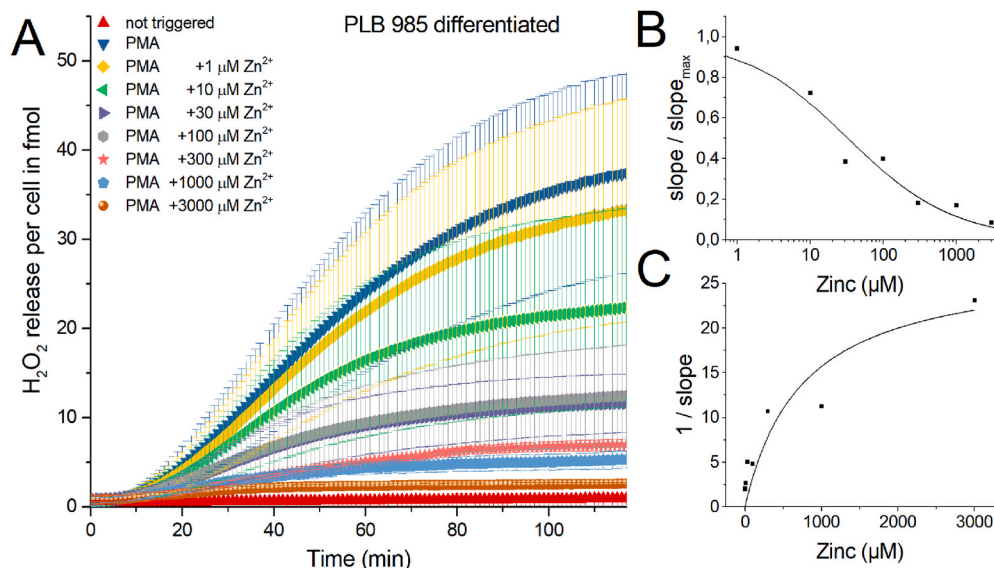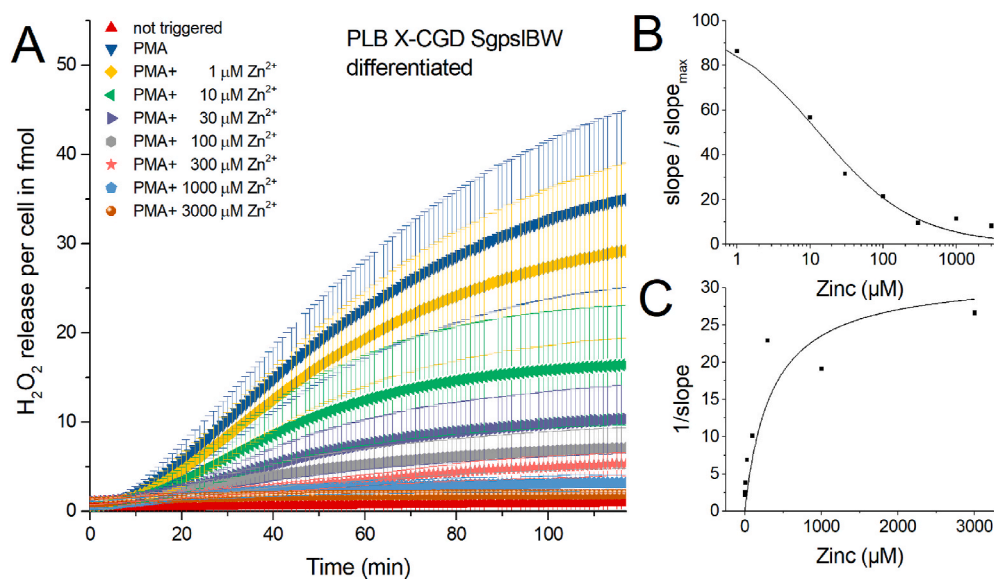**Fig. 1.** H_2O_2 production of human PMN activated by PMA and inhibited by zinc.

A) In seven independent experiments H_2O_2 release was measured over 120 min. Zinc concentrations from 1 μM to 3 mM inhibit H_2O_2 release. Data is displayed as Mean ± SD. Overall release of H_2O_2 is seen at 120 min. Maximal rate of production is determined at the steepest slope of H_2O_2 release over time. Data was normalized to a single cell (n = 7). **B)** Inhibition response curve giving an $IC_{50} = 21$ μM Zn^{2+}. **C)** Dixon Plot fitted with a Michaelis-Menten-Equation showing an apparent $K_M = 799$ μM Zn^{2+}.

Fig. 2. H_2O_2 production of human PLB 985 cells activated by PMA and inhibited by zinc. **A)** In five independent experiments over of 120 min H_2O_2 release was measured. Zinc concentrations from 1 μM to 3 mM inhibited H_2O_2 release. Data is displayed as Mean ± SD. Overall release of H_2O_2 is seen at 120 min. Maximal rate of production is determined at the steepest slope of H_2O_2 release over time. Data was normalized to a single cell (n = 5). **B)** Dose-response curve giving an IC_{50} = 33 μM Zn^{2+}. **C)** Dixon Plot fitted with a Michaelis-Menten-Equation showing an apparent K_M =751 μM Zn^{2+}. Abbreviations: PLBd = PLB cells differentiated, +PMA = triggered by PMA, +1000 μM Zn^{2+} = 1 mM zinc used to inhibit H_2O_2 release.

PLB985 cells, which we attribute to the inhomogeneous differentiation too. In contrast, freshly isolated PMN showed a defined standard error. PMN are fully differentiated as they enter the bloodstream. Therefore, the variance presented in the data would be expected to be less. Based exclusively on the mean H_2O_2 release, zinc inhibits PLB985 cells comparable to PMN (Supp Fig. 1). The amount of reactive oxygen species that originate from the mitochondria instead of the NADPH oxidase might be quantified by using a PLB985 cell line that has the NOX2 gene knocked out. We performed the standard experiment utilizing PLB X-CGD NOX2 knock-out cell line [51]. Measuring the H_2O_2 release over 2 h did not demonstrate any clearly quantifiable amount (Supp Fig. 2), in comparison to the NOX2 originated H_2O_2. We conclude that under the conditions we applied, the majority of H_2O_2 quantified was due to NOX2. Mitochondrial ROS production appeared neglectable (Supp Fig. 2).

In PLB X-CGD SgpslBW (abbreviated = SgpsIBW) cell line NOX2 genetic information was reintroduced into the PLB X-CGD cell line. We ran another five experiments with this rescue cell line (Fig. 3), partly to find out whether a higher expression of NOX2 would enhance ROS production. Quantitatively, we measure almost the same amount of

H_2O_2 released as from the PLB985 cells (Supp Fig. 1).

All three cell types are strongly releasing H_2O_2. Evidently, all cell types start with a delay after PMA activation which is shortest in PMN (PMN < PLB = PLB X-CGD SgpsIBW). A high rate H_2O_2 release is in the first part of the H_2O_2 curve. Usually the maximum release takes place during this phase. The slope (fmol • min^{-1} • $cell^{-1}$) decreases afterwards and over time the respiratory burst is stopped. We assume that an unknown factor is stopping further production of ROS. The shortage of substrate (glucose) as a stopping factor during the respiratory burst is readily excludable. Glucose is converted into NADPH via the hexose monophosphate shunt [55]. Consequently, we may estimate how much glucose is converted into NADPH [56]. Approximately 3.75×10^{13} molecules of glucose are used as substrate in a microplate well that contains 25.000 cells during the respiratory burst. The amount of glucose in the well is 3.00×10^{17} molecules. Therefore, it is unlikely that a lack of substrate is stopping the respiratory burst in phagocytes. Oxygen is estimated to be at a concentration around 200 μM in the well. 10–20 μM of oxygen is maximally consumed during the respiratory burst by the 25000 cells per well. It seems unlikely that oxygen deprivation is a reason for the reduction of H_2O_2 release. Product inhibition by H_2O_2

Fig. 3. H_2O_2 production of human PLB985 X-CGD SgpslBW cells activated by PMA and inhibited by zinc.
A) In five independent experiments H_2O_2 release was measured over 120 min. Zinc concentrations from 1 μM to 3 mM inhibit H_2O_2 release. Data is displayed as Mean ± SD. Overall release of H_2O_2 is seen at 120 min. Maximal rate of production is determined at the steepest slope of H_2O_2 release over time. Data was normalized to a single cell (n = 5). **B)** Dose-response curve giving an IC_{50} = 13 μM Zn^{2+}. **C)** Dixon Plot fitted with a Michaelis-Menten-Equation showing an apparent K_M =350 μM Zn^{2+}. Abbreviations: BWd = PLB X-CGD SgpslBW differentiated, + PMA = triggered by PMA, + 1 μM Zn^{2+} = additional 1 μM zinc in well.

appears to be unlikely too. The release of H_2O_2 into the well is highest in the PMA (control) triggered trace without zinc. The lowest H_2O_2 release is in the PMA +3 mM zinc trace. However, the termination of the respiratory burst in the PMA +3 mM zinc trace is much earlier than in the PMA without zinc trace (control). Consequently, the amount of H_2O_2 released appears not to be the reason for termination. If that were the case, the lower amount of H_2O_2 should have a stronger effect on release.

3.3. Zinc removal experiments

One central question of this study is: Does zinc inhibition affects the phagocytes irreversibly, or does H_2O_2 release continue undisturbed after chelating zinc? Furthermore, if an unknown stopping factor diffuses away after zinc inhibition is released. We generated a highly buffered EGTA containing solution. Zinc is chelated by EGTA with a 1:1 stoichiometry. The stability constant of EGTA and Zinc is higher than for Ca^{2+} and Mg^{2+}, the other divalent ions in our Ringer solution. Hence, EGTA binds preferentially Zn^{2+} over Ca^{2+} and over Mg^{2+}. One other side effect is that if the chelator binds divalent ions, protons are released [57]. Thus pH measurements were performed in Ringer with zinc concentrations from 1 μM to 3000 μM after adding 2 μl EGTA solution. We were able to modify the solution to a point were exclusively a small deviation from the actual ringer pH (pH = 7.4) was achieved. Maximally, the EGTA solution reduced the pH from 7.4 to 7.1. In Fig. 4 zinc removal is shown at an early stage of the H_2O_2 release. Remarkably, the effect of the pH drop is readily seen in the control trace without zinc (blue trace). However, even the comparably small inhibitory effect of 1 μM zinc could be reverted by EGTA to a H_2O_2 release of control + EGTA values. After EGTA addition the traces containing zinc concentrations of 10, 30 and 100 μM drastically increased the release of H_2O_2. A drop in signal was visible minutes after the addition of EGTA. This phenomenon appeared constantly in all recordings after EGTA addition. We suspect some interaction of EGTA with the Amplex Red reagent might be responsible for the drop. However, we are able to exclude automatic calibration of the plate reader since the control traces didn't show an adjustment in the comparable time window. The calibration traces showed a drop of Amplex Red fluorescence due to 2 μl EGTA solution addition but never a rise in signal. We attribute the drop to the slightly lowered pH. Thus we are certain that the increase in H_2O_2 release is a biological signal connected to the cells. The recovery, after EGTA addition, of H_2O_2 release is stronger than the simultaneously run control trace. It appears that at higher concentrations of zinc the recovery due to

EGTA is in total weaker (Fig. 4), even though the peak slope of H_2O_2 release is almost the same (Fig. 4B + 4C) as in control. We suspected that termination of the respiratory burst might be accompanied by cell death of PMN and potentiated by zinc [58]. Removal of zinc by EGTA would remove the inhibition of H_2O_2 release. The peak slope would represent all cells able to continue releasing H_2O_2 uninhibited. Therefore, it should represent the "working/living" fraction of cells. Fig. 4B and C support the hypothesis almost fully. For instance at 10 μM zinc, the zinc inhibited and by EGTA disinhibited cells (green hollow symbols) release almost as much H_2O_2 per time as the 1 μM zinc (yellow hollow symbols) and PMA control trace (blue hollow symbols). However, much more than the still 10 μM zinc inhibited trace (green filled symbols).

EGTA has been tested on PMN granules before [59]. Interestingly, the apparent maximal ROS production was not changed by EGTA, but the oxidation of NADPH was enhanced. The enhanced oxidation of NADPH might be the reason for the irregular curve shapes after EGTA addition. Unfortunately, we weren't able to investigate this phenomenon in more detail. In the calibration curve (without cells) EGTA reduced the signal slightly over time.

Furthermore, the use of a high stability chelator, that complexes free zinc, will never chelate all free zinc. The reaction would predict that between the two binding molecules -proton channel and EGTA-the free zinc will bind and unbind. The higher the initial zinc concentration in the well the higher will be the amount of zinc still able to bind to proton channels after EGTA chelation.

We tested whether chelating zinc at a later point in time (50 min) during the experiment would show comparable data (Supp Fig.4). Here, the recovery of H_2O_2 release after zinc chelation appeared in total diminished compared to the earlier EGTA addition. However, the peak rate of release (slope/$slope_{max}$) (Supp Figs. 4B–C) was close to the data from Fig. 4. At a concentration of 300 μM zinc, a visible decline in release rate manifests during the late application of EGTA, suggesting a smaller contribution of "working/releasing" cells.

The data implies a time dependence of the respiratory burst consisting of three phases/parts. The first phase is the delay representing activation and assembly of the NOX2 complex. The second phase is very stable and characterized by massive H_2O_2 release. The third phase is represented by the decline of H_2O_2 release.

3.4. Analysis of cell death by flow cytometry

The reduced total release of H_2O_2 might be explained by cell death.
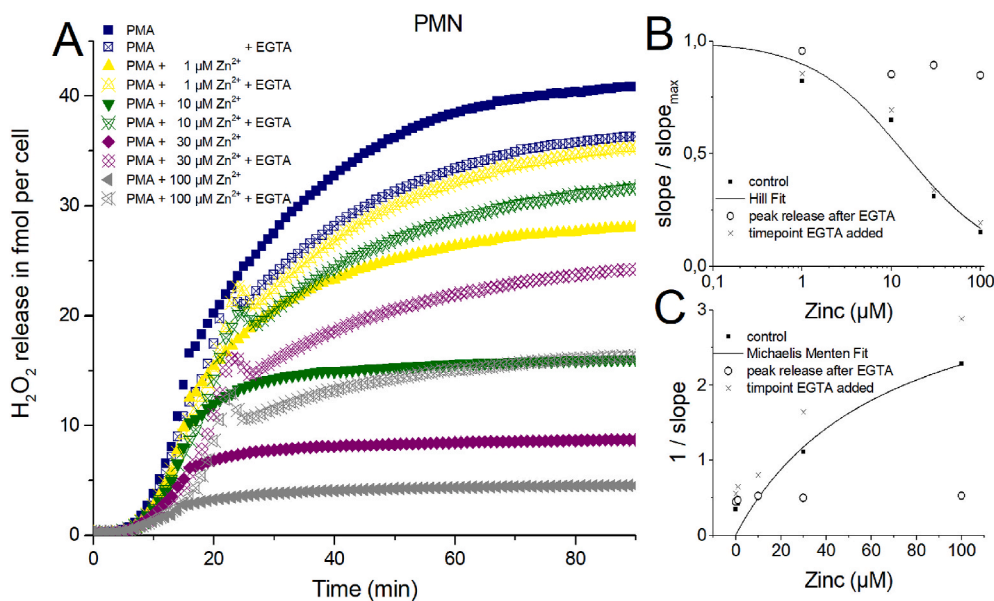
Fig. 4. H_2O_2 release of human PMN inhibited by zinc and chelated by EGTA.
A) In three independent experiments over of 90 min H_2O_2 release was measured. Zinc concentrations from 1 μM to 3 mM inhibit H_2O_2 release. Data is displayed as Mean. EGTA was added at ≈ 16 min. Overall release of H_2O_2 is seen at 90 min. Maximal rate of production is determined at the steepest slope of H_2O_2 release over time. Data was normalized to a single cell. **B)** Dose-response curve giving an IC_{50} = 14 μM Zn^{2+}. **C)** Dixon Plot fitted with a Michaelis-Menten-Equation showing an apparent K_M = 67 μM Zn^{2+}.

We investigated cell death of the two cell lines SgpsIBW (used before in Fig. 3) and the comparable NOX2 knock out cell line SBW by using flow cytometry and the DNA-binding dye propidium iodide (PI). Propidium iodide is a DNA intercalating molecule that is unable to enter the cell if the plasma membrane is still intact. To mimic our H_2O_2 experiments, cells were differentiated for 6 days with DMSO. Cells were incubated at 37 °C for 80 min in an identical Ringer used in all of the presented H_2O_2 releasing measurements. Additionally, the incubation was made with or without PMA and in the presence or absence of zinc, to establish reasonable control experiments. 80 min as point in time was selected in agreement with our H_2O_2 recordings in Fig. 3. Fig. 5 shows the results of three experiments. Zinc was used at four different concentrations: 0, 3, 30, and 300 μM. Both cell lines express Blue Fluorescent Protein (BFP) and are derived from the PLB-X-CGD cell line after lentiviral transduction. SBW cells serve as KO control for the SgpsIBW cells, which additionally over-express a cDNA coding for NOX2. Thus, we set the gates to BFP + cells to directly compare NOX2 non-expressing to NOX2 overexpressing cells. Both cell lines responded to increasing zinc concentrations with enhanced cell death. PMA alone increased the number of dead cells in comparison to control. Our results show that higher zinc concentrations in connection with PMA increase the amount of dead cells. At 300 μM zinc the difference between dead cells in solely zinc and zinc plus PMA is less pronounced. We record zinc and PMA affecting the viability of the cells. Interestingly, 300 μM Zn^{2+} appear to effectively reduce viability even without PMA.

3.5. Mathematical model

This model is based on experimentally obtained data of human PMN and derives from Murphy and DeCoursey [8].

First, we extended the model so that we were able to calculate H_2O_2 production from electron current. In accordance with the stoichiometry of the chemical reactions, two electrons translocated across the membrane to generate one H_2O_2 molecule and one molecular oxygen. Surprisingly, the Murphy model does not reproduce our experimental data. It doesn't terminate the respiratory burst but reaches a constant H_2O_2 rate of release over time. Applying exclusively the Murphy model would *per se* not lead to stoppage of H_2O_2 release (Fig. 6). Therefore, the Murphy Model might be missing an additional factor terminating the H_2O_2 release of PMN. Our investigation of voltage gated proton channel inhibition by zinc [26] enabled us to build a simple model of zinc inhibition by solely reducing the rate constant of proton channel activation. We followed this path and reduced the activation rate constant with increasing zinc concentration in the model. This approach was implemented before by Murphy and DeCoursey. In our model we mimicked the four zinc concentrations we used in our experiments. We wanted to implement a provisional simple approach with which we could reproduce the experimentally acquired H_2O_2 data. Therefore, the electron current has to be close to zero after 120 min of simulation time. This would match the constant H_2O_2 value seen at the end of the experiments with no further H_2O_2 release. We introduced two modifications in the Murphy Model. First, we included a Posicast function [60]. Posicast determines a delay after which the original signal is turned off. We found that a delay of 264–946 s is sufficient to reproduce the experimental data without deviating drastically from the predicted membrane potential (Fig. 8). The second modification was a filter equation that scaled the result to the experimental data. Posicast and filter parameters are shown in Supp. Table 1. We thought that the
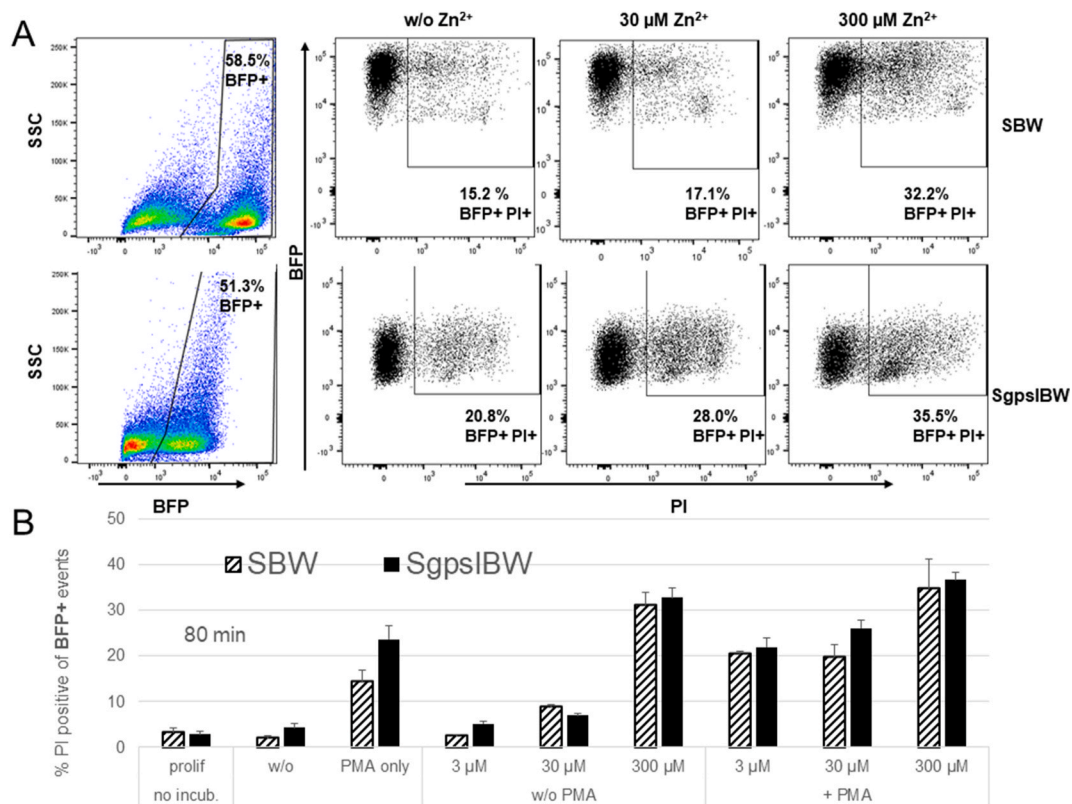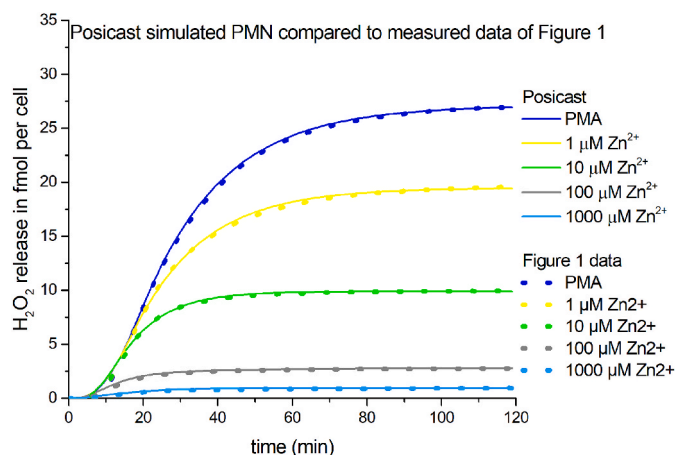

Fig. 5. Zinc and PMA increases cell death during the respiratory burst
A) Dotplots of the two PLB985 cell lines: SBW cells (don not express NOX2) and SgpsIBW cells (do express a functional NADPH oxidase). Gates are set according to the expression of BFP (blue fluorescence protein). Cell death is assessed via the uptake of membrane impermeable PI. Increasing concentrations of zinc lead to more dead cells. **B)** Summary of three individual experiments with 80 min incubation at 37 °C. Data is depicted as Mean + SD. 120 nM PMA increases cell death, which is augmented by rising concentrations of zinc. 300 μM of zinc has an impact on cell viability with and without PMA. Abbreviations: BFP + cells fluorescence blue, PI + cells have taken up PI.
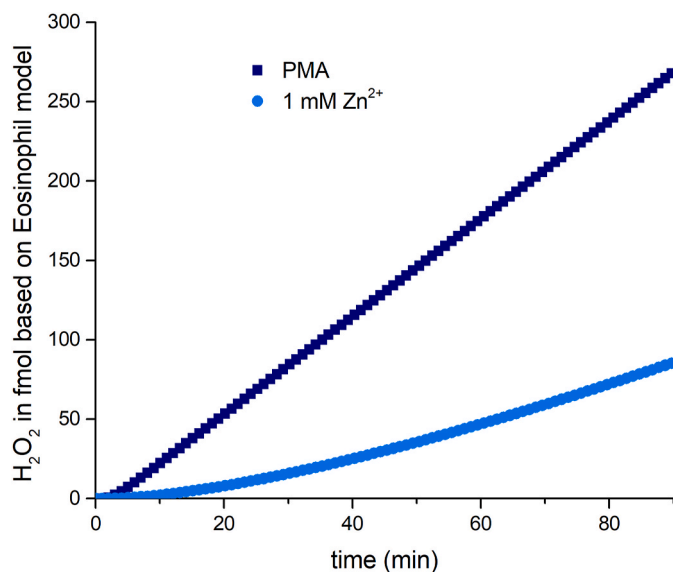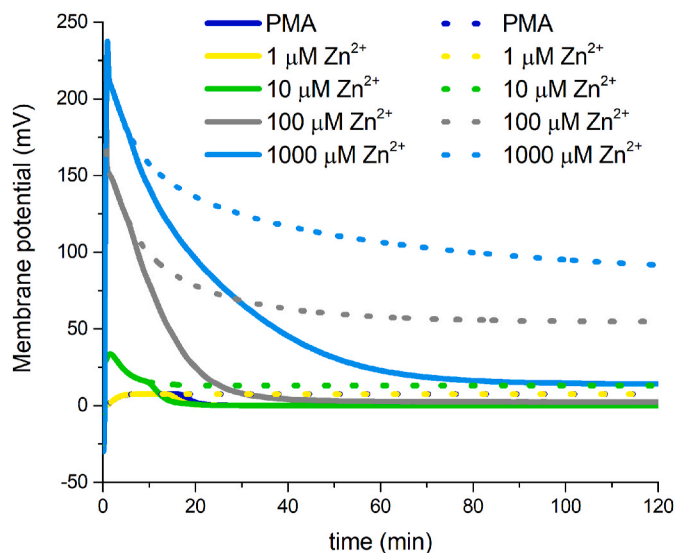
Fig. 6. Model calculation of H_2O_2 release by PMN. Using the model of Murphy and DeCoursey we calculated the H_2O_2 production from the model lasting 90 minutes. The model doesn't predict termination of the H_2O_2 release of PMN. Not even under conditions simulating proton channel inhibition with 1 mM zinc. Corresponding to our experiments the model predicts an initial delay but does not capture the H_2O_2 release correctly over a longer period of time.

Fig. 8. Simulated membrane potential changes in PMN by the Murphy/DeCoursey model and the implemented Posicast/Filter function.
Murphy and DeCoursey model calculated membrane potential changes in dashed lines. Murphy and DeCoursey model modified by the Posicast/Filter equation in straight lines. The initial voltage changes are the same in both approaches. However, in between 10-20 minutes of the simulations membrane potential declines faster due to Posicast/Filter onset.

Posicast function simulates the termination phenomenon of the experiments sufficiently, as can be seen in Fig. 7 overlapping measured data and simulation data. One potential scenario would be that parts of the population of cells start to terminate H_2O_2 release by ultimately entering cell death, throughout the respiratory burst. Consequently, the pool of cells that release H_2O_2 is diminishing. The decline of releasing cells results into a net reduction of overall NADPH activity, hence electron current. Additionally, on single cell level, the Posicast/filter modifications imitate the reduction of electron current by potentially lowered cytosolic pH. Zinc inhibition of proton channels reduces the intracellular pH [18,20]. Strong depolarization decreases the electron current caused by the voltage-dependence of NOX2. Thus, these factors would contribute to lowered H_2O_2 release. Interestingly, the dead time until cutoff of the Posicast correlates well with the observed earlier cessation

of H_2O_2 release at higher zinc concentrations, during the experiments in Fig. 1. Finally, Posicast function is one potential add-on to reproduce zinc inhibition results by using the experimental data based model of Murphy.
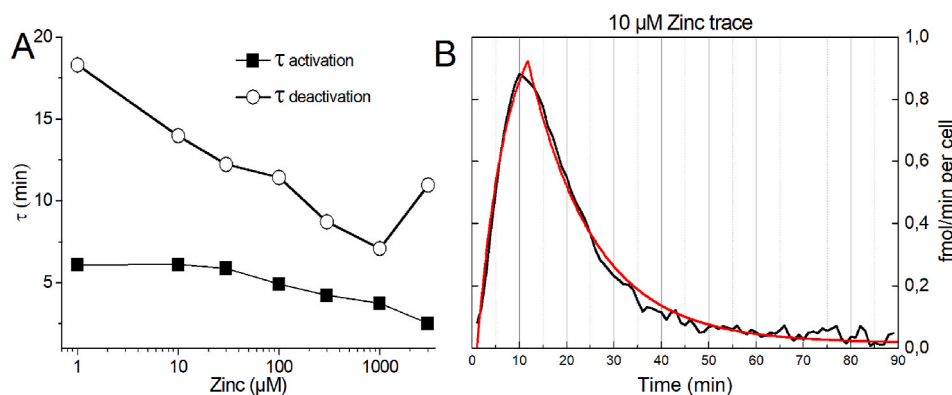
Moreover, we used a second approach. We fitted the first derivative of the H_2O_2 release traces from previous experiments using two first order exponential functions. One, describing the rising part of the first derivative as activation time constant. The other describes the declining part. After analyzing the results, we recognized comparable small changes in the time constant of activation (which is technically difficult to resolve and more an estimate) but pronounced changes in the time constant of deactivation (Fig. 9A). The deactivation time constant appears to be dependent on the zinc concentration. Thus, the time course of respiratory burst termination is mostly dependent on the deactivation time constant which shortens by increasing zinc concentrations. Fig. 9B shows a typical fit of the first derivative of the 10 μM zinc trace (see Fig. 1).

Overall, we present two potential approaches to extract information about the respiratory burst termination from the H_2O_2 release of PMN. Both approaches specifically target the saturating part of the H_2O_2 release due to zinc.

4. Discussion

This study was designed to understand the respiratory burst of human PMN in more detail. Why the respiratory burst terminates and which factor or factors are responsible for the stoppage of ROS release is currently under discussion. We investigated the release of H_2O_2 during the respiratory burst via the well-established Amplex Red assay [61]. Our results suggest that the membrane potential and potentially the cytosolic pH are probable factors that affect the respiratory burst and possibly terminate it.

While we discovered two new potential factors, we might be able to exclude some previously suggested factors to be dominant in terminating the H_2O_2 release due to zinc inhibition.

Fig. 7. Modelled H_2O_2 release by PMN including Posicast/Filter function.
Modifying model of Murphy and DeCoursey we calculated the H_2O_2 production from the modified model lasting 120 minutes. Here, Posicast function reproduces the termination of H_2O_2 release over time. Four zinc concentrations and control are included. Dashed lines represent the recorded PMN data from Fig. 1.

Fig. 9. Fitting the first derivative of H_2O_2 release by two single exponential equations.
A) Time constants $[Zn^{2+}]$ plot, calculated out of the first derivative of the H_2O_2 release. First derivative was fitted with two single exponential equations as in B. Deactivation time constant is stronger dependent on zinc than activation time constant. B) Example of a fit of the first derivative of the 10 µM zinc inhibition H_2O_2 release trace. Note fits were increasingly difficult at high zinc concentrations because of the low signal to noise ratio.

4.1. H_2O_2 does not predominantly inhibit the respiratory burst during zinc inhibition

The cumulative amount of H_2O_2 released is not a factor that ceases the respiratory burst. Reproducibly, higher zinc concentrations change the shape of the resulting H_2O_2 release curve. The point in time when the H_2O_2 release is almost zero appears early with increased zinc concentration. The cumulative maximal release is lower with higher zinc concentrations. As a membrane permeant substance, H_2O_2 would be equally distributed between the volume of the well and the cytosol of the cell. If H_2O_2 accumulates in the cell due to massive release, it would accumulate the most and have the highest impact on those H_2O_2 curves which show the strongest release, but the opposite is the case. The curves that produce the least amount, progress into zero release the earliest. Therefore, H_2O_2 as a dominant termination factor might be excludable during the respiratory burst of PMN and zinc inhibition.

Another possibility is product inhibition due to H_2O_2. High concentrations of H_2O_2 would inhibit the conversion of O_2^- into H_2O_2. Again, this mechanism would predict that the highest H_2O_2 release curves would reach zero accumulation the earliest. We cannot detect such effects in our measurements and therefore we exclude the product inhibition hypothesis.

4.2. Change in phosphorylation as terminator of H_2O_2 release

We are using PMA as the sole activator of the respiratory burst. PMA stimulation appears to be practically irreversible. It induces NADPH oxidase assembly in the surface membrane so that O_2^- is formed in the extracellular solution [43]. In our experiments this is readily measurable with Amplex Red. However, the PMA concentration has an equal concentration in all wells. This implies that termination by changes in phosphorylation status would identically affect the shape of all curves, for both PMA and for PMA + zinc concentrations. This is not the case. Solely, if zinc were to affect PKC by an unknown mechanism, the experimental results could be explained. To our knowledge there is no report of zinc affecting PKC.

4.3. Change of the cytoskeleton terminates H_2O_2 release

In the introduction we mentioned that the actin of the cytoskeleton is one essential component that terminates the respiratory burst. If the pH inside the cytosol is changing, then certainly the NADPH oxidase by itself [18], but also the components of the cytoskeleton, are affected. The pH dependence of the cytoskeleton reduces the cycling rate of NADPH oxidase, determined by assembly and disassembly. This would reduce the number of active oxidase complexes and result in declining H_2O_2 release. Additionally, changes in membrane potential would affect the NADPH oxidase, particularly the transmembrane complexes [19], but should not impact proteins inside the cytosol. Hence, the cytoskeleton is

most likely affected by lower pH but most probably not by membrane potential.

4.4. Membrane potential is terminating the respiratory burst

Several publications report that the activity of the NADPH oxidase depolarizes the membrane potential of phagocytes [62]. Values up to 60 mV have been reported for human neutrophils [63]. Approximating the ordinate of the membrane potential measurements from *Rada* et al. and *Geiszt* et al., to positive values, results in depolarization around +50 mV [3,64]. Zinc amplifies the effect of NADPH oxidase activity on the membrane potential. Depolarizations up to +180 mV under zinc inhibition have been described in granulocytes [65]. The long depolarization over time frames from minutes to hours may result into plasma membrane rupture in phagocytes. Generally, in patch-clamp experiments voltages over +100 mV over seconds tend to result in membrane rupture. Therefore, termination of the respiratory burst might be connected to unsustainability of the inner milieu and subsequent cell death. We introduced a factor into the mathematical model that represents non-functional oxidases (Posicast), and we analyzed the decline of H_2O_2 release depending on zinc concentration. Our model calculates H_2O_2 release curves comparable to our experimental data (Fig. 7), exclusively focussing on membrane potential and zinc inhibition.

4.5. Cytosolic acidification terminates respiratory burst

During the respiratory burst in phagocytes protons are massively produced. The sources for the protons are the oxidation of NADPH to $NADP^+ + H^+$, the hexose monophosphate shunt that generates a proton for each NADPH made, and additionally ½ CO_2 is produced which could be a potential source of a proton in the cytosol. Hence, acidification of the cytosol has to happen during the respiratory burst. The main transporters involved into proton translocation are the voltage-gated proton channel, the sodium proton antiporter, and proton ATPases. It appears that the most energetically efficient way to lower the proton concentration inside the cell is to passively conduct the hydrogen ions through the voltage gated proton channel H_V1. However, the sodium proton antiporter participates in the pH homeostasis too, utilizing the transmembrane sodium gradient. The proton ATPase consumes ATP to translocate the proton and is therefore the most energetically demanding way. Morgan et al. *2009* reported that voltage gated proton channels and sodium proton antiporter are essential to counteract acidification [20]. ATPases take part also but their contribution is comparably small. If acidification is the consequence of the respiratory burst then it is straight forward to suggest massive acidification as a factor that terminates the respiratory burst. The cellular protein machinery is pH-dependent and less efficient the lower the pH inside the cell is. H_V1 knock-out PMN investigated by El Chemaly et al. [36], have shown pH reduction during control conditions and even stronger after a

PMA triggered respiratory burst. Acidification could be a cause for burst termination.

Chemistry predicts that two electrons are needed to generate one molecule H_2O_2. Thus, from the H_2O_2 data we are able to estimate the electron current of a single cell. However, patch–clamp registrations of electron current found that I_e is stable throughout hours or until the measurement is disrupted. Therefore, it is likely that the two components, membrane potential and pH, which are clamped by the patch pipette during patch-clamp recordings, could play a decisive role in respiratory burst termination in PMN. In contrast to patch-clamp recordings, the registrations in well plates do neither clamp the transmembrane potential nor the cytosolic pH.

Our experiments show time dependence when chelating the zinc away from the proton channel generating a recovery of the H_2O_2 release. In an early phase (7–10 min) the recovery due to zinc chelation was substantial while at a late phase (50 min) it showed smaller effects. The steepness of the slope after recovery by late EGTA (50 min) was 50% smaller than at early EGTA addition. Thus, nonfunctional cells or cell death due to zinc inhibition might be the straight forward explanation for this phenomenon.

We ran flow cytometry assays using PI to stain cells with disrupted plasma membrane. PI would not show whether the cell is acidified, depolarized or apoptotic, it plainly shows that the plasma membrane cannot prevent the entrance of the dye into the nucleus. Thus, it might not reflect all cells that stop releasing H_2O_2 but those which are not able to keep the internal milieu. Both zinc and PMA kill cells. Zinc alone at low concentrations isn't very effective. Cell death is triggered strongest by PMA in combination with increasing zinc concentrations. However, we see a comparable effect with the cell line that has NOX2 knocked out. The PMA effect on the NOX2 k. o. cell line is smaller than on the cell line harboring the reintroduced NOX2. We checked undifferentiated cells of both cell lines. Both showed much less cell death than differentiated cells triggered with PMA and inhibited by zinc (Supp Fig.5), suggesting that there is a dependence on maturation. Both NOX2 and H_V1 are more expressed, generate more ROS, and conduct more protons during maturation of HL-60 cells [54,66]. Thus, the result encourages a connection to those two proteins but does not completely exclude other factors that are upregulated during maturation. The high amount of dead cells in the NOX2 knock-out suggests that other PMA triggered effects might contribute to cell death and these are somewhat zinc sensitive.

4.6. Cell death as consequence of the respiratory burst

There is vast literature covering PMN cell death. An impressive amount of studies investigated which stimuli are enhancing or delaying cell death. Here, in this study, we are using PMA, an activator of PKC. Our flow cytometry assays show cell death dependent on maturation, NOX2 expression and zinc concentration, underlining cell death as a consequence of the respiratory burst.

We are observing function of the cells by measuring the release of H_2O_2. Zinc compromises this function substantially in a dose dependent fashion. The key experiment to prove this is the removal of zinc by the chelator EGTA. If this is done at an early point in time during the respiratory burst, then function can be restored to almost control value. But later in the respiratory burst, the chelation of zinc has just minimal effect on restoring the cell function. Comparing the kinetics of the H_2O_2 production reveals that the termination of the respiratory burst is faster with higher zinc concentrations. Some "factor or factors" have to be responsible for this termination. Zinc inhibits H_V1 at low $[Zn^{2+}]$. Membrane potential and cytosolic pH are directly modulated by H_V1 during the respiratory burst. Both may most certainly result in a multitude of subsequent processes in PMN. Low intracellular pH has been shown to enhance caspase activity [67], PMA has been shown to induce cell death in PMN [68–70]. Depolarization is an early molecular event in cell death [71,72], and volume changes in a living cells are very

much dependent on the transmembrane potential [73,74].

### 4.7. High zinc concentrations affecting other immune cells than PMN

In short, not only the respiratory burst of PMN is affected by zinc ions. There are reports of natural killer cells which show suppressed killing activity by high zinc concentrations. In the adaptive immune system, high zinc concentrations attenuate and suppress T cell function, and B cells undergo apoptosis in high zinc concentrations [75,76]. However, in these cells the effect of zinc might differ from the proposed mechanism above and was not investigated in this study.

5. Conclusion

In this work we have shown that NOX2 and H_V1 are the main proteins contributing to zinc inhibition of the respiratory burst in PMN. PLB985 derived cell lines, as well as freshly isolated human PMN, responded similarly to zinc inhibition. Freshly isolated PMN are a more homogenous population of cells than differentiated PLB985 cells. We found that cell death might be the continuation of the termination of the respiratory burst. Termination is rapid at high zinc concentrations but it appears also in control experiments, albeit much later. During the respiratory burst chelating zinc by EGTA recovers H_2O_2 release drastically in the early phase of the experiment, while in the late phase recovery is diminished. Our additions to the mathematical model allow a qualitative estimation of H_2O_2 production by PMN and a first approximation of the time constants underlying burst termination. To our knowledge EGTA chelating experiments and the improved mathematical model are first shown in this publication. Our data reinforce the hypothesis that termination of the respiratory burst by zinc is accelerated and might be dependent on membrane potential, intracellular pH and followed by cell death (Fig. 10). Lastly, free zinc has a substantial impact on immune cell function. Thus, this study hopefully underscores its importance in life sciences.

Author contributions

AD and GC did H_2O_2 experiments, data analysis, cell culture, cell isolation and produced figures. SS and MS provided the PLB985 cell
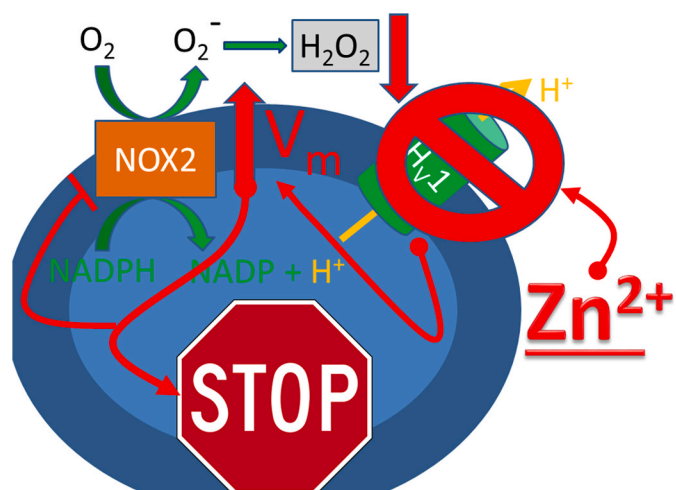
Fig. 10. Schematic drawing of a PMN affected by Zn^{2+}.
The PMN represented as blue oval, terminates (stops) its respiratory burst by zinc inhibition of the voltage-gated proton channel H_V1. The further effects of zinc are depicted in red. Zinc directly binds to H_V1 and inhibits proton conduction, leading to a rise in the membrane potential (V_m). The highly elevated V_m inhibits NOX2, which is inhibited by increased transmembrane voltage. Subsequently, H_2O_2 release declines. Therefore, high $[Zn^{2+}]$ dampens the respiratory burst of PMN and leads to termination of the burst.

lines and cell culture support. AT and SS performed flow cytometry experiments, analyzed data and generated figures, HK transferred and extended the mathematical model of Murphy and DeCoursey and fitted the first derivatives. BM analyzed data and wrote the paper.

Funding

Declaration of competing interest

All the authors declare that the research was conducted in the absence of any commercial or financial relationships that could be construed as a potential conflict of interest.

Acknowledgments

Appendix A. Supplementary data

Supplementary data to this article can be found online at https://doi.org/10.1016/j.redox.2021.102133.

References

[1] C.A. Janeway Jr., Approaching the asymptote? Evolution and revolution in immunology, Cold Spring Harbor Symp. Quant. Biol. 54 (Pt 1) (1989) 1–13.

[2] L. Du Pasquier, The immune system of invertebrates and vertebrates. Comparative biochemistry and physiology Part B, Biochem. Mol. Biol. 129 (2001) 1–15.

[3] B.K. Rada, M. Geiszt, K. Kaldi, C. Timar, E. Ligeti, Dual role of phagocytic NADPH oxidase in bacterial killing, Blood 104 (2004) 2947–2953.

[4] K. Bedard, K.H. Krause, The NOX family of ROS-generating NADPH oxidases: physiology and pathophysiology, Physiol. Rev. 87 (2007) 245–313.

[5] W.M. Nauseef, How human neutrophils kill and degrade microbes: an integrated view, Immunol. Rev. 219 (2007) 88–102.

[6] C.C. Winterbourn, M.B. Hampton, J.H. Livesey, A.J. Kettle, Modeling the reactions of superoxide and myeloperoxidase in the neutrophil phagosome: implications for microbial killing, J. Biol. Chem. 281 (2006) 39860–39869.

[7] C.C. Winterbourn, A.J. Kettle, Redox reactions and microbial killing in the neutrophil phagosome, Antioxidants Redox Signal. 18 (2013) 642–660.

[8] R. Murphy, T.E. DeCoursey, Charge compensation during the phagocyte respiratory burst, Biochim. Biophys. Acta 1757 (2006) 996–1011.

[9] B. Musset, S.M. Smith, S. Rajan, D. Morgan, V.V. Cherny, T.E. DeCoursey, Aspartate [112] is the selectivity filter of the human voltage-gated proton channel, Nature 480 (2011) 273–277.

[10] V.V. Cherny, V.S. Markin, T.E. DeCoursey, The voltage-activated hydrogen ion conductance in rat alveolar epithelial cells is determined by the pH gradient, J. Gen. Physiol. 105 (1995) 861–896.

[11] I. Kovacs, M. Horvath, T. Kovacs, K. Somogyi, L. Tretter, M. Geiszt, G.L. Petheo, Comparison of proton channel, phagocyte oxidase, and respiratory burst levels between human eosinophil and neutrophil granulocytes, Free Radic. Res. 48 (2014) 1190–1199.

[12] G.L. Petheő, A. Orient, M. Baráth, I. Kovács, B. Réthi, A. Lányi, A. Rajki, E. Rajnavőlgyi, M. Geiszt, Molecular and functional characterization of H_V1 proton channel in human granulocytes, PloS One 5 (2010) e14081.

[13] Y. Okochi, Y. Aratani, H.A. Adissu, N. Miyawaki, M. Sasaki, K. Suzuki, Y. Okamura, The voltage-gated proton channel Hv1/VSOP inhibits neutrophil granule release, J. Leukoc. Biol. 99 (2016) 7–19.

[14] Y. Okochi, M. Sasaki, H. Iwasaki, Y. Okamura, Voltage-gated proton channel is expressed on phagosomes, Biochem. Biophys. Res. Commun. 382 (2009) 274–279.

[15] T.E. DeCoursey, V.V. Cherny, W. Zhou, L.L. Thomas, Simultaneous activation of NADPH oxidase-related proton and electron currents in human neutrophils, Proc. Natl. Acad. Sci. U. S. A. 97 (2000) 6885–6889.

[16] B. Musset, V.V. Cherny, T.E. DeCoursey, Strong glucose dependence of electron current in human monocytes, Am. J. Physiol. Cell Physiol. 302 (2012) C286–C295.

[17] T.E. DeCoursey, V.V. Cherny, Temperature dependence of voltage-gated H^+ currents in human neutrophils, rat alveolar epithelial cells, and mammalian phagocytes, J. Gen. Physiol. 112 (1998) 503–522.

[18] D. Morgan, V.V. Cherny, R. Murphy, B.Z. Katz, T.E. DeCoursey, The pH dependence of NADPH oxidase in human eosinophils, J. Physiol. 569 (2005) 419–431.

[19] T.E. DeCoursey, D. Morgan, V.V. Cherny, The voltage dependence of NADPH oxidase reveals why phagocytes need proton channels, Nature 422 (2003) 531–534.

[20] D. Morgan, M. Capasso, B. Musset, V.V. Cherny, E. Rios, M.J. Dyer, T.E. DeCoursey, Voltage-gated proton channels maintain pH in human neutrophils during phagocytosis, Proc. Natl. Acad. Sci. U. S. A. 106 (2009) 18022–18027.

[21] S. Grinstein, W. Furuya, Cytoplasmic pH regulation in phorbol ester-activated human neutrophils, Am. J. Physiol. 251 (1986) C55–C65.

[22] T.E. DeCoursey, Voltage-gated proton channels find their dream job managing the respiratory burst in phagocytes, Physiology 25 (2010) 27–40.

[23] J.K. Femling, V.V. Cherny, D. Morgan, B. Rada, A.P. Davis, G. Czirjak, P. Enyedi, S. K. England, J.G. Moreland, E. Ligeti, W.M. Nauseef, T.E. DeCoursey, The antibacterial activity of human neutrophils and eosinophils requires proton channels but not BK channels, J. Gen. Physiol. 127 (2006) 659–672.

[24] M.P. Mahaut-Smith, The effect of zinc on calcium and hydrogen ion currents in intact snail neurons, J. Exp. Biol. 145 (1989) 455–464.

[25] C. Jardin, G. Chaves, B. Musset, Assessing structural determinants of Zn^{2+} binding to human H_V1 via multiple MD simulations, Biophys. J. 118 (2020) 1221–1233.

[26] G. Chaves, S. Bungert-Plumke, A. Franzen, I. Mahorivska, B. Musset, Zinc modulation of proton currents in a new voltage-gated proton channel suggests a mechanism of inhibition, FEBS J. 287 (22) (2020) 4996–5018.

[27] V. De La Rosa, A.L. Bennett, I.S. Ramsey, Coupling between an electrostatic network and the $Zn(2+)$ binding site modulates Hv1 activation, J. Gen. Physiol. 150 (2018) 863–881.

[28] F. Qiu, A. Chamberlin, B.M. Watkins, A. Ionescu, M.E. Perez, R. Barro-Soria, C. Gonzalez, S.Y. Noskov, H.P. Larsson, Molecular mechanism of Zn2+ inhibition of a voltage-gated proton channel, Proc. Natl. Acad. Sci. U. S. A. 113 (2016) E5962–E5971.

[29] V.V. Cherny, T.E. DeCoursey, pH-dependent inhibition of voltage-gated H^+ currents in rat alveolar epithelial cells by Zn^{2+} and other divalent cations, J. Gen. Physiol. 114 (1999) 819–838.

[30] G.L. Petheo, N. Demaurex, Voltage- and NADPH-dependence of electron currents generated by the phagocytic NADPH oxidase, Biochem. J. 388 (2005) 485–491.

[31] M.B. Sorensen, I.A. Bergdahl, N.H. Hjollund, J.P. Bonde, M. Stoltenberg, E. Ernst, Zinc, magnesium and calcium in human seminal fluid: relations to other semen parameters and fertility, Mol. Hum. Reprod. 5 (1999) 331–337.

[32] H. Pang, X. Wang, S. Zhao, W. Xi, J. Lv, J. Qin, Q. Zhao, Y. Che, L. Chen, S.J. Li, Loss of the voltage-gated proton channel Hv1 decreases insulin secretion and leads to hyperglycemia and glucose intolerance in mice, J. Biol. Chem. 295 (2020) 3601–3613.

[33] Z.A. Karcioglu, Zinc in the eye, Surv. Ophthalmol. 27 (1982) 114–122.

[34] B.L. Vallee, Zinc: biochemistry, physiology, toxicology and clinical pathology, Biofactors 1 (1988) 31–36.

[35] N. Demaurex, A. El Chemaly, Physiological roles of voltage-gated proton channels in leukocytes, J. Physiol. 588 (2010) 4659–4665.

[36] A. El Chemaly, Y. Okochi, M. Sasaki, S. Arnaudeau, Y. Okamura, N. Demaurex, VSOP/Hv1 proton channels sustain calcium entry, neutrophil migration, and superoxide production by limiting cell depolarization and acidification, J. Exp. Med. 207 (2010) 129–139.

[37] M. Chvapil, L. Stankova, D.S. Bernhard, P.L. Weldy, E.C. Carlson, J.B. Campbell, Effect of zinc on peritoneal macrophages in vitro, Infect. Immun. 16 (1977) 367–373.

[38] H. Laggner, K. Phillipp, H. Goldenberg, Free zinc inhibits transport of vitamin C in differentiated HL-60 cells during respiratory burst, Free Radical Biol. Med. 40 (2006) 436–443.

[39] L. Stankova, G.W. Drach, T. Hicks, C.F. Zukoski, M. Chvapil, Regulation of some functions of granulocytes by zinc of the prostatic fluid and prostate tissue, J. Lab. Clin. Med. 88 (1976) 640–648.

[40] J. Yatsuyanagi, T. Ogiso, Zinc inhibition of respiratory burst in zymosan-stimulated neutrophils: a possible membrane action of zinc, Chem. Pharm. Bull. 36 (1988) 1035–1040.

[41] N.Z. Gammoh, L. Rink, Zinc in infection and inflammation, Nutrients 9 (2017).

[42] R. Zhao, K. Kennedy, G.A. De Blas, G. Orta, M.A. Pavarotti, R.J. Arias, J.L. de la Vega-Beltran, Q. Li, H. Dai, E. Perozo, L.S. Mayorga, A. Darszon, S.A.N. Goldstein, Role of human Hv1 channels in sperm capacitation and white blood cell respiratory burst established by a designed peptide inhibitor, Proc. Natl. Acad. Sci. U. S. A. 115 (2018) E11847–E11856.

[43] T.E. DeCoursey, E. Ligeti, Regulation and termination of NADPH oxidase activity, Cell. Mol. Life Sci. 62 (2005) 2173–2193.

[44] A.J. Jesaitis, J.O. Tolley, R.G. Painter, L.A. Sklar, C.G. Cochrane, Membrane-cytoskeleton interactions and the regulation of chemotactic peptide-induced activation of human granulocytes: the effects of dihydrocytochalasin B, J. Cell. Biochem. 27 (1985) 241–253.

[45] P. Moskwa, M.C. Dagher, M.H. Paclet, F. Morel, E. Ligeti, Participation of Rac GTPase activating proteins in the deactivation of the phagocytic NADPH oxidase, Biochemistry 41 (2002) 10710–10716.

[46] G.M. Bokoch, B.A. Diebold, Current molecular models for NADPH oxidase regulation by Rac GTPase, Blood 100 (2002) 2692–2696.

[47] J.T. Curnutte, R.W. Erickson, J. Ding, J.A. Badwey, Reciprocal interactions between protein kinase C and components of the NADPH oxidase complex may regulate superoxide production by neutrophils stimulated with a phorbol ester, J. Biol. Chem. 269 (1994) 10813–10819.

[48] A. Boyum, Isolation of mononuclear cells and granulocytes from human blood. Isolation of monuclear cells by one centrifugation, and of granulocytes by combining centrifugation and sedimentation at 1 g, Scand. J. Clin. Lab. Invest. Suppl. 97 (1968) 77–89.

[49] C. Immerwahr, Beiträge zur Kenntnis der Löslichkeit von Schwermetall-Niederschlägen auf elektrochemischem Wege, Zeitschrift für Elektrochemie 7 (1901) 477–483.

[50] K.A. Tucker, M.B. Lilly, L. Heck Jr., T.A. Rado, Characterization of a new human diploid myeloid leukemia cell line (PLB-985) with granulocytic and monocytic differentiating capacity, Blood 70 (1987) 372–378.

[51] L. Zhen, A.A. King, Y. Xiao, S.J. Chanock, S.H. Orkin, M.C. Dinauer, Gene targeting of X chromosome-linked chronic granulomatous disease locus in a human myeloid leukemia cell line and rescue by expression of recombinant gp91phox, Proc. Natl. Acad. Sci. U. S. A. 90 (1993) 9832–9836.

[52] C. Brendel, K.B. Kaufmann, A. Krattenmacher, S. Pahujani, M. Grez, Generation of X-CGD cells for vector evaluation from healthy donor CD34(+) HSCs by shRNA-mediated knock down of gp91(phox), Mol. Ther. Methods Clin. Develop. 1 (2014), 14037.

[53] D.R. Ambruso, B.G. Bolscher, P.M. Stokman, A.J. Verhoeven, D. Roos, Assembly and activation of the NADPH:O2 oxidoreductase in human neutrophils after stimulation with phorbol myristate acetate, J. Biol. Chem. 265 (1990) 924–930.

[54] J. Hua, T. Hasebe, A. Someya, S. Nakamura, K. Sugimoto, I. Nagaoka, Evaluation of the expression of NADPH oxidase components during maturation of HL-60 cells to neutrophil lineage, J. Leukoc. Biol. 68 (2000) 216–224.

[55] N. Borregaard, J.H. Schwartz, A.I. Tauber, Proton secretion by stimulated neutrophils. Significance of hexose monophosphate shunt activity as source of electrons and protons for the respiratory burst, J. Clin. Invest. 74 (1984) 455–459.

[56] A. Jankowski, S. Grinstein, Modulation of the cytosolic and phagosomal pH by the NADPH oxidase, Antioxidants Redox Signal. 4 (2002) 61–68.

[57] P. Djurdjevic, J. Bjerrum, L. Melander, U. Wahlgren, C. Watt, Metal ammine formation in solution. XXIV. The copper(II)– and some other metal(II)–Mono- and diethanolamine systems, Acta Chem. Scand. 37a (1983) 881–890.

[58] R.J. Coakley, C. Taggart, N.G. McElvaney, S.J. O'Neill, Cytosolic pH and the inflammatory microenvironment modulate cell death in human neutrophils after phagocytosis, Blood 100 (2002) 3383–3391.

[59] M.B. Goetz, R.A. Proctor, Effect of chelating agents and superoxide on human neutrophil NAD(P)H oxidation, Anal. Biochem. 137 (1984) 230–235.

[60] Smith OJM: Posicast control of damped oscillatory systems, Proc. IRE 45 (1957) 1249–1255.

[61] J.G. Mohanty, J.S. Jaffe, E.S. Schulman, D.G. Raible, A highly sensitive fluorescent micro-assay of H2O2 release from activated human leukocytes using a dihydroxyphenoxazine derivative, J. Immunol. Methods 202 (1997) 133–141.

[62] F. Di Virgilio, P.D. Lew, T. Andersson, T. Pozzan, Plasma membrane potential modulates chemotactic peptide-stimulated cytosolic free Ca2+ changes in human neutrophils, J. Biol. Chem. 262 (1987) 4574–4579.

[63] A. Jankowski, S. Grinstein, A noninvasive fluorimetric procedure for measurement of membrane potential. Quantification of the NADPH oxidase-induced depolarization in activated neutrophils, J. Biol. Chem. 274 (1999) 26098–26104.

[64] M. Geiszt, A. Kapus, K. Nemet, L. Farkas, E. Ligeti, Regulation of capacitative Ca2+ influx in human neutrophil granulocytes. Alterations in chronic granulomatous disease, J. Biol. Chem. 272 (1997) 26471–26478.

[65] N. Demaurex, G.L. Petheő, Electron and proton transport by NADPH oxidases, Philos. Trans. R. Soc. Lond. B Biol. Sci. 360 (2005) 2315–2325.

[66] A.Y. Qu, A. Nanda, J.T. Curnutte, S. Grinstein, Development of a H+-selective conductance during granulocytic differentiation of HL-60 cells, Am. J. Physiol. 266 (1994) C1263–C1270.

[67] S. Matsuyama, J. Llopis, Q.L. Deveraux, R.Y. Tsien, J.C. Reed, Changes in intramitochondrial and cytosolic pH: early events that modulate caspase activation during apoptosis, Nat. Cell Biol. 2 (2000) 318–325.

[68] K. Suzuki, H. Namiki, Phorbol 12-myristate 13-acetate induced cell death of porcine peripheral blood polymorphonuclear leucocytes, Cell Struct. Funct. 23 (1998) 367–372.

[69] T. Saito, H. Takahashi, H. Doken, H. Koyama, Y. Aratani, Phorbol myristate acetate induces neutrophil death through activation of p38 mitogen-activated protein kinase that requires endogenous reactive oxygen species other than HOCl, Biosci. Biotechnol. Biochem. 69 (2005) 2207–2212.

[70] H. Takei, A. Araki, H. Watanabe, A. Ichinose, F. Sendo, Rapid killing of human neutrophils by the potent activator phorbol 12-myristate 13-acetate (PMA) accompanied by changes different from typical apoptosis or necrosis, J. Leukoc. Biol. 59 (1996) 229–240.

[71] C.D. Bortner, M. Gomez-Angelats, J.A. Cidlowski, Plasma membrane depolarization without repolarization is an early molecular event in anti-Fas-induced apoptosis, J. Biol. Chem. 276 (2001) 4304–4314.

[72] R. Franco, C.D. Bortner, J.A. Cidlowski, Potential roles of electrogenic ion transport and plasma membrane depolarization in apoptosis, J. Membr. Biol. 209 (2006) 43–58.

[73] C.M. Armstrong, The Na/K pump, Cl ion, and osmotic stabilization of cells, Proc. Natl. Acad. Sci. U. S. A. 100 (2003) 6257–6262.

[74] J.A. Fraser, C.L. Huang, A quantitative analysis of cell volume and resting potential determination and regulation in excitable cells, J. Physiol. 559 (2004) 459–478.

[75] K.H. Ibs, L. Rink, Zinc-altered immune function, J. Nutr. 133 (2003) 1452S–1456S.

[76] A.H. Shankar, A.S. Prasad, Zinc and immune function: the biological basis of altered resistance to infection, Am. J. Clin. Nutr. 68 (1998) 447S–463S.